Title: Rapid one pot synthesis of Xanthene derivatives by an efficient and reusable nano $ZnAl_2O_4$ - an insight into a new process

Author: Triveni Rajashekhar Mandlimath Balijapalli Umamahesh Kulathu I. Sathiyanarayanan

PII: S1381-1169(14)00168-X
DOI: http://dx.doi.org/doi:10.1016/j.molcata.2014.04.030
Reference: MOLCAA 9092

To appear in: *Journal of Molecular Catalysis A: Chemical*

Received date: 6-2-2014
Revised date: 21-4-2014
Accepted date: 22-4-2014

Please cite this article as: T.R. Mandlimath, B. Umamahesh, K.I. Sathiyanarayanan, Rapid one pot synthesis of Xanthene derivatives by an efficient and reusable nano $ZnAl_2O_4$ - an insight into a new process, *Journal of Molecular Catalysis A: Chemical* (2014), http://dx.doi.org/10.1016/j.molcata.2014.04.030

Rapid one pot synthesis of Xanthene derivatives by an efficient and reusable nano $ZnAl_2O_4$ - an insight into a new process

Triveni Rajashekhar Mandlimath, Balijapalli Umamahesh and Kulathu I. Sathiyanarayanan*

Chemistry Division – School of Advanced Sciences

VIT University, Vellore – 632014, Tamil Nadu, India

Highlights

- Synthesis of nano $ZnAl_2O_4$ by [metal citrate]-acrylamide polymer precursor method.
- The nano $ZnAl_2O_4$ nanoparticles were hexagonal-like with 20 nm in size.
- Nano $ZnAl_2O_4$ had 50 m^2/g surface area and total surface acidity of 8.8 mmol NH_3/g.
- The nano spinel oxide was an excellent catalyst for the synthesis of xanthenes.
- We recycled the catalyst for 10 cycles with consistent activity.

Abstract

Nano $ZnAl_2O_4$ was synthesized by blending metal-citrate complex-acrylamide polymer using the precursor method. Powder X- ray diffraction analysis of the catalyst affirmed that the spinel oxide was phase pure. Elemental analysis was confirmed by Energy Dispersive X-ray analysis. Transmission Electron Microscopic (TEM) analysis and Scherrer's formula revealed that the particles were found to be in the order of 20 nm in size. Thermal stability of the catalyst was analyzed by thermogravimetric and differential thermal analysis (TG-DTA). Total acidity of the nano $ZnAl_2O_4$ evaluated by NH_3-TPD was 8.8 mmol NH_3/g. Diversity in the synthesis of xanthene derivatives was investigated using nano zinc aluminate as a catalyst. Nanoform of the catalyst showed better activity than the bulk form due to its large surface area 50 m^2/g. The 2,2'-arylmethylene bis (3-hydroxy-2cyclohexene-1-one), 2,2'-arylmethylene bis (3-hydroxy-5,5-dimethyl-2cyclohexene-1-one) and 1-Oxo-hexahydroxanthenes were synthesized rapidly using $ZnAl_2O_4$ and the catalyst was successfully recycled without any loss of activity.

Key words: nano $ZnAl_2O_4$, TEM, 1-Oxo-hexahydroxanthene

*** Corresponding author - Kulathu I. Sathiyanarayanan** Fax: +914162243092
E-mail: sathiya_kuna@hotmail.com

1. Introduction

$ZnAl_2O_4$ (Ghanite), a normal spinel oxide with AB_2O_4 structure, is one of the most important aluminates investigated in literature due to its charismatic properties such as high thermal and chemical stability, high mechanical resistance, ductility, low sintering temperature. The structure

crystallizes in cubic system in which Zn^{2+} ion occupies tetrahedral sites and octahedral sites by Al^{3+} ion. This has been widely studied by several researchers for diverse applications. For instance, cobalt doped $ZnAl_2O_4$ proved as a blue pigment with good chromaticity [1]. Ghanite acts as a host lattice for several transition metals and rare earth ions, enhancing the photoluminescent properties such as green light emitting $ZnAl_2O_4$: Mn, red light emitting Eu^{3+} doped $ZnAl_2O_4$, green light emitting Tb^{3+} doped $ZnAl_2O_4$ and yellow light emitting Dy^{3+} doped $ZnAl_2O_4$ [2- 4].

The catalytic behavior of $ZnAl_2O_4$ has been extensively investigated for a variety of organic reactions: $ZnAl_2O_4$ nanoparticle is an excellent catalyst for the acetylation of amines, alcohols and phenols at room temperature [5]. Sr(II)-$ZnAl_2O_4$ acts as an efficient catalyst for the oxidation of various alcohols [6]. Palladium nanoparticles immobilized on microporous $ZnAl_2O_4$ has been studied for Suzuki-Miyaura coupling reaction to achieve high yield within short period [7]. Apart from the liquid phase reactions, Ghanite has also been used for gas phase hydroxylation of 2-hydroxypyridine, gas phase transformation of anisole to cresol and gas phase alkylation of m-cresol [8-10]. In addition to these, $ZnAl_2O_4$ has been used as a potential catalyst for photodegradation of gaseous toluene, photooxidation of toluene and lanthanum doped Ghanite for biodiesel preparation from soyabean oil. Oxidation of light alkanes has been catalyzed using Ru/$ZnAl_2O_4$ and Pt/$ZnAl_2O_4$, Ni/$ZnAl_2O_4$-CeO_2 for hydrogen production from ethanol steam and Pt-Sn/ $ZnAl_2O_4$ for Propane dehydrogenation [11- 18].

Xanthene derivatives are fascinating organic compounds with vast applications in pharmacology because of their anti-inflammatory, antibacterial, antifungal, anti-depressant and antimalarial activity [19-21]. They are thrombin inhibitors, and also act as stimulants of the central nervous system [22, 23]. These compounds are potassium channel openers [24] and

possess anticancer activity [25]. Apart from its biological applications, xanthene dyes have been used for diagnostic and imaging applications [26]. Benzopyran derivatives possess anti-inflammatory, anti-analgesic and antimicrobial properties [27]. They act as insulin sensitizers [28]. The compounds having benzopyran rings function as potential potassium channel activators [29], and also active towards post-coital contraceptives [30].

Condensation of aromatic aldehydes with cyclic 1,3-diketones is one of the methods to synthesize 2,2'-arylmethylene bis (3-hydroxy-2-cyclohexene-1-one), 2,2'-arylmethylene bis (3-hydroxy-5,5-dimethyl-2-cyclohexene-1-one) and 1-Oxo-hexahydroxanthenes. Traditional method for synthesizing these compounds involves the use of piperidine as catalyst [31]. This method has a major drawback because piperidine cannot be recycled. Synthesis of 2,2'-arylmethylene bis (3-hydroxy-2-cyclohexene-1-one) and 2,2'-arylmethylene bis (3-hydroxy-5,5-dimethyl-2-cyclohexene-1-one) derivatives have been reported using NaOH under high intensity ultrasound radiation [32] and urea under ultrasound radiation [33]. These methods may not be applicable for large scale production, and further the catalysts cannot be reused. Several homogeneous catalysts such as $ZnCl_2$, ethylenediamine diacetate (EDDA), $SmCl_3$, SDS, CsF and heterogeneous catalysts like ZnO, $Yb(OTf)_3$-SiO_2, $FeCl_3.6H_2O$/TMSCl/[bmim][BF_4], $HClO_4$-SiO_2 and L-Lysine have been reported by various authors [34-42]. However, many of these catalysts are expensive, require toxic solvents, cannot be recycled and require prolonged duration.

1-Oxo-hexahydroxanthene has been synthesized by Sabitha et al. using $CeCl_3.7H_2O$ [43]. Although this protocol tends to give better yields, the catalyst is expensive, non-reusable, and needs long reaction time. Pesyan et al. have used acetic acid for the synthesis of 1-Oxo-hexahydroxanthenes [44]. Kuarm et al. attempted the use of cellulose sulfuric acid as catalyst

[45]. The catalyst requires acid for its preparation. Fei He et al. have performed the synthesis of 1-Oxo-hexahydroxanthenes using glycerol [46]. Even though it is a catalyst-free synthesis, it requires prolonged refluxing to achieve the products. Apart from these, various homogeneous catalysts such as cationic surfactant triethylbenzylammoium chloride (TEBA), TCT and tetra-n-butylammonium fluoride (TBAF) and PTSA have been reported for the synthesis [47-50]. In spite of showing catalytic activity, few of these catalysts are halogen containing, active only in the presence of toxic solvents, and also need prolonged reaction time.

In the present work, we report the synthesis of nano $ZnAl_2O_4$ using [metal citrate complex]-acrylamide polymer precursor method and the investigation of its catalytic activity for the synthesis of 2,2'-arylmethylene bis (3-hydroxy-2cyclohexene-1-one), 2,2'-arylmethylene bis (3-hydroxy-5,5-dimethyl-2-cyclohexene-1-one) and 1-Oxo-hexahydroxanthenes by Knoevenagel condensation followed by Micheal addition of aromatic aldehydes with cyclic 1,3-diketones. Diversity in the synthesis of xanthenes derivatives has been studied using nano $ZnAl_2O_4$.

2. Experimental Work

Zinc nitrate ($Zn(NO_3)_2.6H_2O$, 99%), Aluminium nitrate ($Al(NO_3)_3.9H_2O$, 99%) were purchased from Himedia. Citric acid monohydrate ($C_6H_{10}O_8$, 99.99%), acrylamide (C_3H_5NO, 99%), N, N'-methylenebisacrylamide ($C_7H_{10}N_2O_2$, 99%), aldehydes and diketones were purchased from Sigma Aldrich.

2.1. Preparation of bulk $ZnAl_2O_4$

Stoichiometric quantities of $Zn(NO_3)_2.6H_2O$ and $Al(NO_3)_3.9H_2O$ were separately dissolved in distilled water. The metal nitrate solutions were mixed together under constant stirring. The

114 homogenized solution mixture was dried at 80 °C overnight to get the solid mass. The obtained
115 precursor was then calcined at 700 °C for 12 h with a heating rate of 10 °C/ min.

116 **2.2. Preparation of nano $ZnAl_2O_4$**

117 Stoichiometric quantities of $Zn(NO_3)_2$. $6H_2O$ and $Al(NO_3)_3.9H_2O$ were separately dissolved in
118 distilled water. The metal nitrate solutions were added drop wise to the citric acid solution under
119 constant stirring. The ratio of [Zn+Al] and citric acid was 1. To the above homogeneous
120 solution, 3 g of acrylamide and N, N'- methylenbisacrylamide were added. The temperature was
121 raised to 80 °C followed by the addition of a pinch of ammonium peroxodisulphate. The
122 obtained white gel was dried overnight at 80 °C to get the solid mass. The solid precursor was
123 later calcined at 300 °C, 500 °C and 700 °C for 6 h at each stage with a heating rate of 10 °C/
124 min.

125 **2.3. Catalytic investigation of $ZnAl_2O_4$**

126 In a typical procedure, aromatic aldehyde (1 mmol), 1,3-diketone (1,3-cyclohexanedion/5,5-
127 dimethyl-1,3-cyclohexanedione) (2 mmol) and calculated amount of catalyst bulk /nano $ZnAl_2O_4$
128 along with 5 mL solvent were placed in a round bottom flask fitted with reflux condenser. The
129 mixture was then heated at 80 °C. Completion of the reaction was monitored by thin layer
130 chromatography (TLC). The catalyst was removed by filtration, and was washed twice with
131 acetone. It was dried at 60 °C in oven for 3 h and used for further cycle. Xanthene derivatives
132 were obtained by re-crystallization in ethanol-THF. Schemes 1 and 2 represent the synthesis of
134 xanthene derivatives using $ZnAl_2O_4$.

136

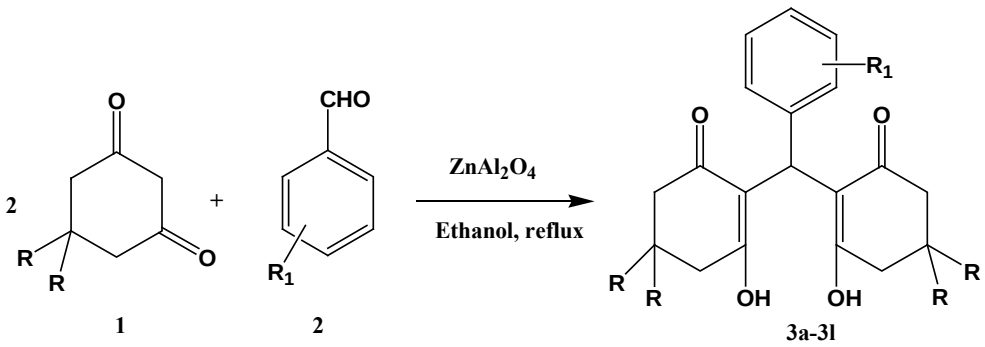

1 2 3a-3l

6

Scheme 1. Synthesis of 2,2'-arylmethylene bis (3-hydroxy-2-cyclohexene-1-one) and 2,2'-arylmethylene bis (3-hydroxy-5,5-dimethyl-2-cyclohexene-1-one)

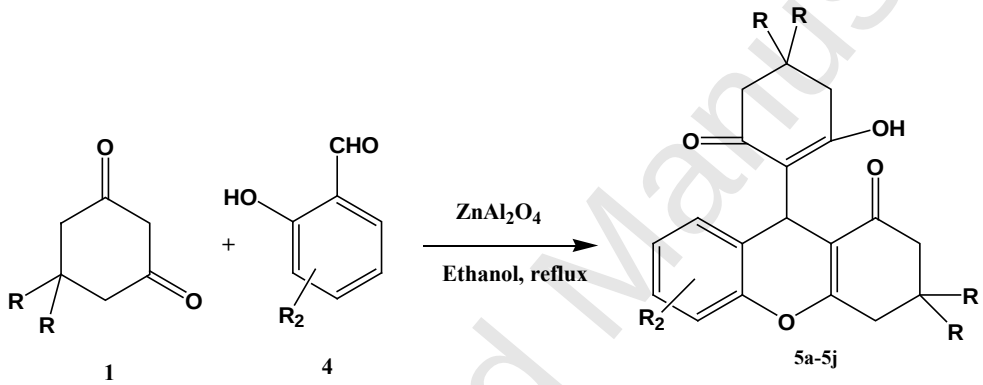

Scheme 2. Synthesis of 1-Oxo-hexahydroxanthene

2.4. Characterization

Phase identification of the catalyst was obtained by powder X-ray diffractometer (Bruker, D8 Advanced) using Cu Kα radiation (λ = 1.5406 Å) in the angle range of 2θ = 10 ° - 70 ° at room temperature. The surface area of the powder samples was analyzed by BET method on Micromeritics ASAP 2020 V3.00 H instrument. Fourier Transformed Infrared Spectra (FTIR) of the prepared samples was recorded on Shimadzu IR affinity – 1 FTIR spectrometer by KBr disk method. The morphology and particle size were affirmed by TEM (JEOL 3010 instrument with UHR pole piece). The particles' size was calculated by using image J software. Elemental

analysis of the catalyst was confirmed by Field Emission Scanning Electron Microscope coupled with Energy Dispersive X-ray Analysis (FESEM-EDX, JEOL JSM 7001F with BRUKER-QUNTAX Version 1.8.2). Thermal analysis of the powder precursor was performed on TA Instrument (SDT Q600) in the temperature range between room temperature and 1000 ºC with the heating rate of 20 ºC per minute. Total surface acidity of the nano $ZnAl_2O_4$ was evaluated by NH_3 temperature-programmed desorption, TPD technique (Autochem 2910, Micromeritics instrument). 0.74 g of the sample was heated to 120 ºC at 10 ºC/min in 30 mL high pure Helium flow, kept at 120 ºC for 30 min. 10% NH_3 in Helium gas at 30 mL/min flow was passed through the sample for 30 min. Pure Helium was purged (30 mL/min) and then desorption of NH_3 was analyzed from 120 ºC to 700 ºC at 10 ºC/min using thermal conductivity detector. Surface basicity of the nano $ZnAl_2O_4$ was analyzed by CO_2 temperature-programmed desorption, TPD technique on the same instrument. In a typical procedure, 1.00 g of the dried sample was pretreated at 200 ºC in 50 mL high pure Helium flow for 30 min. After pretreatment the sample was saturated with 10% CO_2 in Helium gas at 30 ºC (with a flow rate of 75 mL/min). Later Helium was flushed at 105 ºC over the sample for 2 h in order to remove physisorbed CO_2. TPD analysis was done from ambient temperature to 750 ºC at 10 ºC/min. Concentration of leached metal ions from the catalyst during recycle was tested by Atomic Absorption Spectroscopic technique using Varian AA240 instrument. The synthesized Xanthene derivatives were analyzed by ^{1}H NMR and ^{13}C NMR spectra (Bruker FT NMR – 400 MHz).

3. Results and discussion

3.1. Characterization of the catalyst

3.1.1. Powder XRD

Powder XRD patterns of the calcined bulk and nano $ZnAl_2O_4$ are depicted in Fig. 1a. and 1b. Both bulk and nano $ZnAl_2O_4$ are crystallized in face centered cubic structure. The powder XRD patterns were indexed based on ICDD data (# 821043). No impurity peaks were found. Fig 1a consists of narrow peaks, which is apparently bulk $ZnAl_2O_4$. Whereas, the broadening of XRD peaks in Fig. 1b. indicates the formation of nano $ZnAl_2O_4$. The average crystallite size of both bulk and nano $ZnAl_2O_4$ were obtained from the Scherrer's formula ($D = 0.9\lambda/B \cos\theta$) by introducing full width half maximum (FWHM) values of all the peaks in the XRD pattern. 'D' is the average particle size, 'λ' is wavelength of X-ray beam used, 'B' is full width half maximum of the peak and 'θ' is the Bragg angle. The average crystallite size of bulk and nano $ZnAl_2O_4$ was found to be 5 μm and 16 nm respectively. It is apparent from Fig. 2a. and 2b. that the nano $ZnAl_2O_4$ exists even after the 10^{th} cycle.

3.1.2. Mechanism of formation of nanosize $ZnAl_2O_4$

There are 3 different steps involved in the formation of smaller size particles.

i) Metal salts form metal-citrate complex with citric acid.

ii) Monomer acrylamide and cross linker N, N'- methylenbisacrylamide undergo polymerization in the presence of radical initiator ammonium peroxodisulphate giving rise to a polymer network. Thus, Metal citrate persists inside the polymer matrix as shown in the scheme 3.

iii) The [metal-citrate complex]-polymer matrix undergoes decomposition after calcinations and the polymer matrix hinder the growth of particles to larger size and also avoids agglomeration of particles.

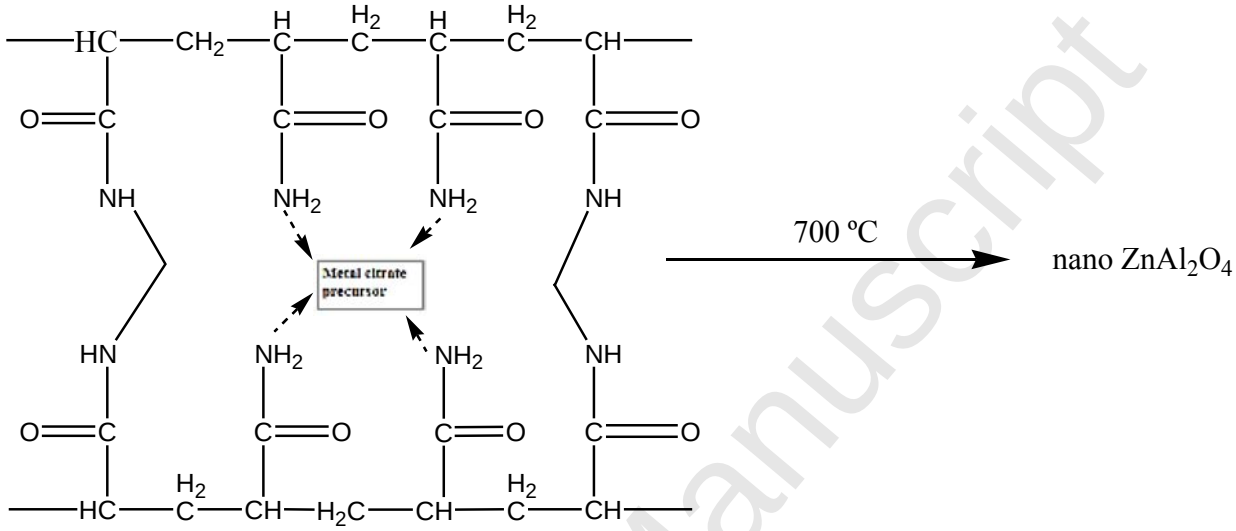

Scheme 3. Mechanism of formation of nano $ZnAl_2O_4$

3.1.3. BET Surface area

Surface area of bulk and nano $ZnAl_2O_4$ from Nitrogen adsorption desorption isotherms obtained by BET method was found to be 10.4 m^2/g and 50 m^2/g respectively.

3.1.4. FTIR Analysis

Figures 3a. and 3b. show FTIR spectrum of bulk and nano $ZnAl_2O_4$. In both the spectra, the bands at 663 cm^{-1}, 559 cm^{-1} and 501 cm^{-1} were assigned to stretching and bending mode of Al-O of octahedral AlO_6 units respectively. Since the characteristic stretching vibration bands of inverse spinel units (AlO_4) in the range 700-850 cm^{-1} were absent, it was clear that the prepared $ZnAl_2O_4$ was pure with normal spinel structure [51]. In case of nano $ZnAl_2O_4$, the peaks at 1630

226 cm^{-1} and 1122 cm^{-1} were assigned to OH stretching of the adsorbed water molecule and
227 asymmetric stretching vibrations of AlO-OH respectively. These two peaks were absent in the
228 FTIR spectrum of bulk $ZnAl_2O_4$. This is because nano $ZnAl_2O_4$ possesses relatively large surface
229 area (50 m^2/g) inclined to adsorb larger number of water molecules over its surface. Also, the
230 possibility of greater number of low coordination site (O^{2-}) over the surface of $ZnAl_2O_4$ cannot
231 be ruled out.

232 **3.1.5. TEM analysis**

233 Figure 4. indicates the TEM image of the prepared nano $ZnAl_2O_4$, which reveals that the nano
234 $ZnAl_2O_4$ particles exhibit hexagonal - like morphology, and are well dispersed. TEM image
235 shows that the particles have a uniform morphology. It is clear that the particles' size is in the
236 range of 5 nm - 20 nm, which corroborates the average particle size obtained from the Scherrer's
237 formula (16 nm). Figure 4 shows the electron diffraction rings, which are indexed as cubic
238 $ZnAl_2O_4$ structure. Particle size distribution is represented in Fig. 5. Maximum size of the
239 particle ranged from 14 to 16 nm.

240 **3.1.6. Energy Dispersive X-ray Analysis (EDX)**

241 The presence of elements Zn, Al and O are confirmed by EDX spectrum (Fig. 6). It was found
242 that theoretical wt % of the elements closely matched with the experimental values.

243 **3.1.7. Thermal Analysis**

244 The compiled TGA and DTA curves of $ZnAl_2O_4$ precursor are shown in Figure. 7. Thermo
245 gravimetric profile revealed that the precursor underwent thermal degradation in two stages. The
246 first weight loss occurred between 50 °C and 120 °C corresponding to the dehydration of

precursor. The second stage of mass loss between 340 °C and 460 °C can be attributed to the decomposition of organic molecules from the precursor. The mass loss from 460 °C to 1000 °C was due to the evolution of entrapped organic molecules in the internal cavities, channels [52]. The weight losses observed from TGA curve was confirmed by the appearance of two endothermic peaks in the same region of the DTA profile.

3.1.8. NH_3-TPD and CO_2-TPD Analysis

Total surface acidity of the nano $ZnAl_2O_4$ evaluated by NH_3-TPD analysis was 8.8 mmol NH_3/g. It was very clear from the NH_3-TPD pattern (Fig. 8) that the broad peaks at 239 °C and 370 °C were associated with weak acidic and medium acidic sites of the material respectively, whereas, the peak at 599 °C was related to strong acidic site. Intensity of broad peaks indicates that the larger distribution of weak and medium acidic sites than the strong acidic sites.

Surface basicity was analyzed by CO_2-TPD. From CO_2-TPD analysis (Fig. 9) it was found that there were no prominent CO_2 desorption peaks and thus the presence of basic sites was ruled out.

3.2. Catalytic Studies of $ZnAl_2O_4$

3.2.1. Synthesis of 2,2'-arylmethylene bis(3-hydroxy-2-cyclohexene-1-one) and 2,2′-arylmethylene bis(3-hydroxy-5,5-dimethyl-2-cyclohexene-1-one)

A mixture of benzaldehyde (1 mmol), 1,3-diketone (1,3-cyclohexanedion/5,5-dimethyl-1,3-cyclohexanedione) (2 mmol) and appropriate amount of catalyst along with 5 mL ethanol were refluxed for few minutes. In general, the mechanism of the formation of xanthenediones involves 2 steps: Knoevenagel condensation followed by Michael addition reaction with cyclization. But surprisingly, the reaction is terminated at the Michael addition step and ended up

with uncylized products (3) within few minutes of using nano $ZnAl_2O_4$ (Scheme 4). Irrespective of the derivatives of benzaldehyde, similar observations were noticed. There was no formation of xanthenediones (3a) even after refluxing the reaction mixture for few hours. Formations of similar products were noticed using both bulk and nano $ZnAl_2O_4$. But nano was found to be more active than bulk catalyst. Since these compounds are pharmacologically very significant, we carried out the reaction with benzaldehyde derivatives and the findings are tabulated in Table.1. Similar observation was made by Malek et al. using ZnO [38]. It is very important to note that the authors achieved the product in 8-15 h of refluxing in CH_3CN solvent.

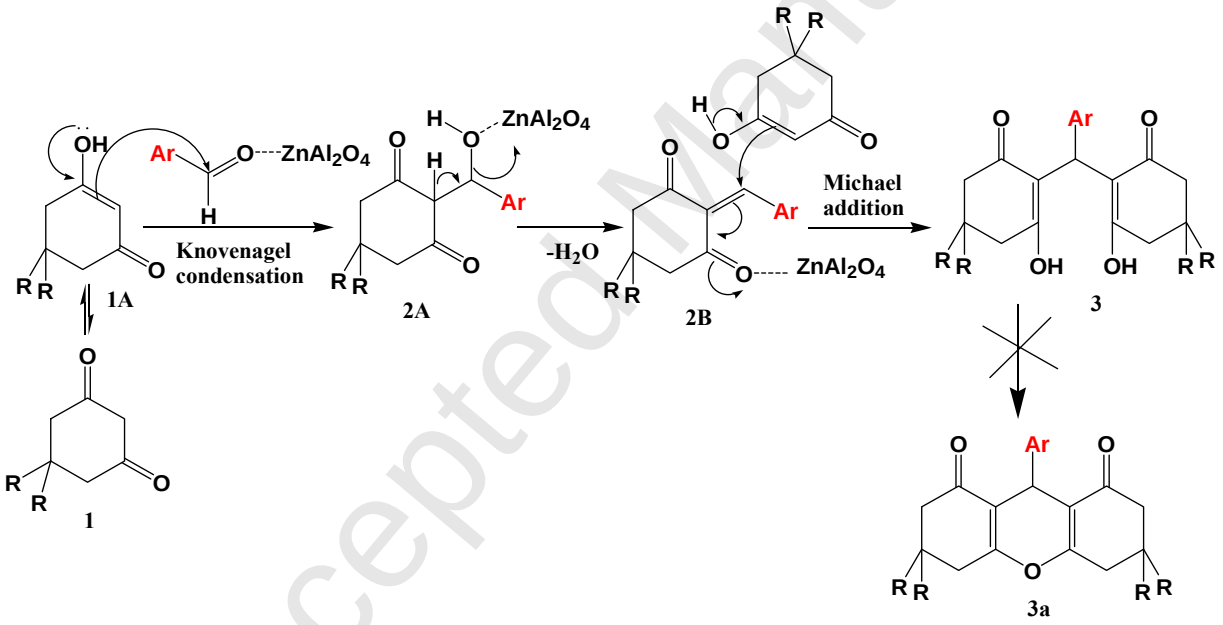

Scheme 4. Plausible mechanism of the formation of uncyclized products.

3.2.2. Synthesis of 1-Oxo-hexahydroxanthene

A mixture of salicylaldehyde (1 mmol), 1,3-diketone (1,3-cyclohexanedion/5,5-dimethyl-1,3-cyclohexanedione) (2 mmol) and appropriate amount of catalyst along with 5 mL ethanol were refluxed for few minutes. Surprisingly, 1-Oxo-hexahydroxanthene formed within few

minutes (Scheme 5). We performed reactions for the other derivatives of salicylaldehyde (Table 2) and obtained 1-Oxo-hexahydroxanthene.

We carried out the synthesis of uncylized products as well as 1-Oxo-hexahydroxanthene without using a catalyst, under similar reaction conditions, and found that the uncyclized product formed after 1 h whereas the latter was formed after 2 h. Consequently, the requirement of catalyst for the synthesis played a crucial role. Here, $ZnAl_2O_4$ accelerated the reaction by bringing both the reactants together over its surface. Table 3. describes the advantage of using nano $ZnAl_2O_4$ over bulk $ZnAl_2O_4$. Due to the small size particles possessing larger surface area (50 m^2/g), nano exhibited better activity than the bulk catalyst whose surface area was 10.4 m^2/g. A Plausible mechanism of 1-Oxo-hexahydroxanthene formation is shown in scheme 5.

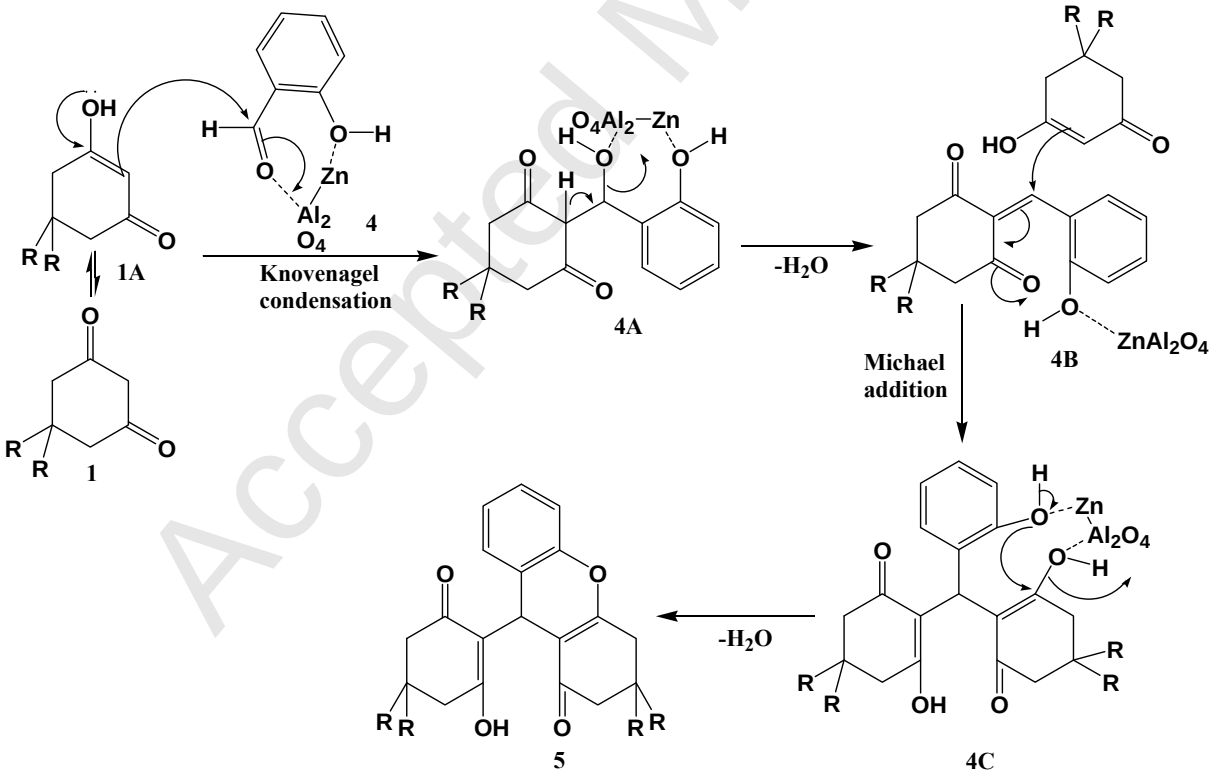

Scheme 5. Plausible mechanism of formation of 1-Oxo-hexahydroxanthene

During the synthesis of 2,2'-arylmethylene bis(3-hydroxy-2-cyclohexene-1-one), 2,2′-arylmethylene bis(3-hydroxy-5,5-dimethyl-2-cyclohexene-1-one) and 1-Oxo-hexahydroxanthene, carbonyl group of the aldehyde interacted with the acidic sites (Zn^{2+} and Al^{3+}) of the catalyst thereby activated the carbonyl carbon for the nucleophilic attack and thus accelerated the reaction. Formation of xanthenediones (3a) generally required high acidic catalyst for the cyclization of product (3). But due to the larger number of weak and medium acidic sites on the surface of nano $ZnAl_2O_4$, the reaction was terminated at uncyclized product (3). The reaction proceeded due to the presence of only acidic sites as the catalyst did not exhibited basic sites.

It was observed that both benzaldehyde and salicylaldehyde derivatives containing electron withdrawing group gave relatively higher yield in short duration (Table 1 and 2). Several authors have reported the synthesis of 1-Oxo-hexahydroxanthene from salicylaldehyde in which they utilized hazardous solvents [49], expensive homogeneous catalysts such $CeCl_3.7H_2O$ and TEBA [43][47], TBAF [49] and it also required longer duration to obtain the products [47-49]. We have made a comparison of the activity of the several catalysts for the synthesis 1-Oxo-hexahydroxanthene with nano $ZnAl_2O_4$ (Table 4). Although the reported homogeneous catalysts produced good yields (Table 4), they contain halogen, very expensive, could not be reused and also took hours for the completion of reaction. Hence nano $ZnAl_2O_4$ could be the best alternative catalyst for the synthesis of 1-Oxo-hexahydroxanthene over the reported homogeneous catalysts.

Next, the effect of solvents for 1-Oxo-hexahydroxanthene synthesis was studied (shown in Table 5). The reaction is found to be faster in protic solvents with high yield. A mere 50 mg of the catalyst gave 86% yield. By increasing the amount of catalyst, the yield obtained was more

and also the reaction time was shortened (Table 6). The reaction was completed in 15 min in the presence of 90 mg of nano $ZnAl_2O_4$, whereas, it completed in 90 min in the presence of 50 mg catalyst. After every cycle, the catalyst was collected by filtration and washed with acetone to remove organic molecules. The catalyst was dried at 60 °C in oven before using it for the next cycle. Nano $ZnAl_2O_4$ was found to be consistently active for 10 cycles as shown in Fig. 10. The yield was reduced after 5 cycles due to the loss of negligible amount of catalyst during filtration. The filtrate collected after each cycle was subjected to AAS analysis for leachability. Leachability of Zn was nil, and hence same was true for Al too. This could be the reason for the consistent performance of catalyst in every cycle.

4. Conclusion

Pure phase of nano $ZnAl_2O_4$ was successfully synthesized by using metal-citrate by polymer precursor method. Particles were found to be in the order of 20 nm size. Nano $ZnAl_2O_4$ was utilized as catalyst for the synthesis of 2,2'-arylmethylene bis(3-hydroxy-2-cyclohexene-1-one), 2,2′-arylmethylene bis(3-hydroxy-5,5-dimethyl-2-cyclohexene-1-one) and 1-Oxo-hexahydroxanthenes. Non-toxic ethanol was used as solvent. We achieved xanthene derivatives with high yields within few minutes. No column chromatography was required. The catalyst was recycled for 5 times without loss of activity. Being non-toxic, inexpensive, highly stable, $ZnAl_2O_4$ emerged as an efficient catalyst, exhibiting diversity in its activity.

4.1. Spectral data of selected xanthene derivatives

4.1.1. Compound 3g (Sl. No. 7 in table 1)

White solid; Melting point: 192 °C, ^{1}H NMR (400 MHz, $CDCl_3$) ppm: 1.10 (s, 6H), 1.23 (s, 6H), 2.48-2.29 (m, 8H), 5.54 (s, 1H), 7.10-7.09 (d, J = 4 Hz, 2H), 7.19-7.15 (t, J = 8 Hz, 1H),

7.28-7.25 (m, 2H), 11.09 (bs s, 2H); ^{13}C NMR (100 MHz, $CDCl_3$) ppm: 27.4, 29.7, 32.8, 46.5, 47.1, 115.6, 115.9, 125.8, 126.8, 128.2, 138.1, 189.4, 190.5.

4.1.2. Compound 5b (Sl. No. 2 in table 2)

Yellow solid; Melting point: 229 °C, ^{1}H NMR (400 MHz, $CDCl_3$) ppm: 1.86-1.75 (m, 2H), 2.17-2.00 (m, 4H), 2.86-2.37 (m, 6H), 3.89 (s, 3H), 4.63 (s, 1H), 6.61-6.59 (d, J = 8 Hz, 2H), 6.77-6.75 (d, J = 8 Hz, 1H), 6.96-6.92 (t, J = 8 Hz, 1H), 10.80 (bs s, 1H); ^{13}C NMR (100 MHz, $CDCl_3$) ppm: 19.7, 19.9, 28.0, 28.0, 29.7, 36.0, 37.0, 56.1, 110.3, 112.2, 119.7, 119.8, 124.3, 125.6, 140.5, 146.9, 170.9, 172.8, 197.1, 201.5.

4.1.3. Compound 5c (Sl. No. 3 in table 2)

Off white solid; Melting point: 221 °C, ^{1}H NMR (400 MHz, $CDCl_3$) ppm: 1.47-1.44 (t, J = 6 Hz, 3H), 2.17-1.82 (m, 6H), 2.85-2.37 (m, 6H), 4.14-4.09 (m, 2H), 4.62 (s, 1H), 6.60-6.58 (d, J = 8 Hz, 1H), 6.76-6.74 (d, J = 8 Hz, 1H), 6.93-6.89 (t, J = 8 Hz, 1H), 10.80 (bs s, 1H); ^{13}C NMR (100 MHz, $CDCl_3$) ppm: 14.9, 19.6, 20.0, 28.0, 28.0, 29.7, 36.0, 37.0, 65.0, 112.1, 112.2, 119.7, 119.9, 124.2, 125.6, 140.9, 146.3, 171.0, 172.6, 197.0, 210.5.

4.1.4. Compound 5f (Sl. No. 6 in table 2)

White solid; Melting point: 203 °C, ^{1}H NMR (400 MHz, $CDCl_3$) ppm: 0.98 (s, 3H), 0.99 (s, 3H), 1.02 (s, 3H), 1.12 (s, 3H), 2.01-1.91 (q, J = 48.0, 16 Hz, 2H), 2.37-2.33 (d, J = 16.0 Hz, 4H), 2.62-2.45 (q, J = 48.0, 16.0 Hz, 2H), 4.67 (s, 1H), 7.03-6.98 (m, 3H), 7.26-7.13 (m, 1H), 10.48 (bs s, 1H); ^{13}C NMR (100 MHz, $CDCl_3$) ppm: 26.5, 27.2, 27.8, 29.2, 29.8, 30.9, 32.3, 41.6, 43.2, 49.9, 50.6, 111.0, 115.7, 118.3, 124.3, 124.6, 127.5, 128.0, 151.0, 169.1, 170.7, 196.6, 200.9.

4.1.5. Compound 5h (Sl. No. 8 in table 2)

Off white solid; Melting point: 170 °C, ^{1}H NMR (400 MHz, $CDCl_3$) ppm: 0.99 (s, 6H), 1.03 (s, 3H), 1.12 (s, 3H), 1.48-1.44 (t, *J* = 8 Hz, 3H), 2.02-1.92 (q, *J* = 44.0, 20.0 Hz, 2H), 2.37-2.33 (m, 4H), 2.69-2.65 (d, *J* = 16.0 Hz, 1H), 2.58-2.54 (d, *J* = 16.0 Hz, 1H), 4.14-4.08 (m, 2H), 4.66 (s, 1H), 6.59-6.57 (d, *J* = 8 Hz, 1H), 6.76-6.74 (d, *J* = 8 Hz, 1H), 6.93-6.89 (t, *J* = 8.0 Hz, 1H), 10.46 (bs s, 1H); ^{13}C NMR (100 MHz, $CDCl_3$) ppm: 14.9, 18.5, 26.5, 27.1, 27.8, 29.2, 29.9, 30.9, 32.3, 41.5, 43.2, 49.9, 50.6, 64.9, 110.8, 112.2, 118.2, 119.8, 124.2, 125.2, 141.1, 146.5, 169.0, 170.5, 196.6, 201.0.

Acknowledgements

Triveni Rajashekhar Mandlimath and B. Umamahesh thank CSIR for providing Senior Research Fellowship. The DST-FIST NMR facility at VIT University is greatly acknowledged. The authors thank Dr. D.Rajan Babu, Professor, SAS, VIT University India and Dr. P. Anandan, RIE Shizuoka University, Hamamatsu, Japan for recording FESEM and EDX. The authors acknowledge M. Sathish Kumar for his help and suggestions.

Appendix. Supplementary data

Supplementary data associated with this article can be found, in the online version at http://dx.doi.org/xxxxxxxxxx

References

[1] L.K.C.D. Souza, J.R. Zamian, G.N.D.R. Filho, L.E.B. Soledade, I.M.G.D. Santos, A.G. Souza, T. Scheller, R.S. Angelica, C.E.F.D Costa, Dyes Pigm. 81 (2009) 187-192.

[2] V. Singh, R.P.S. Chakradhar, J.L. Rao, D.K. Kim, J. Lumin. 128 (2008) 394-402.

[3] B.S. Barros, P.S. Melo, R.H.G.A. Kiminami, A.C.F.M. Costa, G.F.D. Sa, S. Alves Jr, J. Mater. Sci. 41 (2006) 4744-4748.

[4] S.F. Wang, F. Gu, M.K. Lu, X.F. Cheng, W.G. Zou, G.J. Zhou, S.M. Wang, Y.Y. Zhou, J. Alloys Compd. 394 (2005) 255-258.

[5] S. Farhadi, S. Panahandehjoo, Appl. Catal. A. 382 (2010) 293-302.

[6] R.T. Kumar, N.C.S. Selvam, C. Ragupathi, L.J. Kennedy, J.J. Vijaya, Powder Technol. 224 (2012) 147-154.

[7] M. Fang, G.Fan, F. Li, Catal Lett. 2013. DOI 10.1007/s10562-013-1127-y.

[8] H. Grabowska, M. Zawadzki, L. Syper, Appl. Catal. A. 314 (2006) 226-232.

[9] H. Grabowska, M. Zawadzki, L. Syper, Appl. Catal. A. 265 (2004) 221-227.

[10] H. Grabowska, W. Mista, J. Trawczynski, J. Wrzyszcz, M. Zawadzki, Appl. Catal. A. 220 (2001) 207-213.

[11] X. Li, Z. Zhu, Q. Zhao, L. Wang, J. Hazard. Mater. 186 (2011) 2089-2096.

[12] Z. Zhu, Q. Zhao, X. Li, Y. Li, C. Sun, G. Zhang, Y. Cao, Chem. Eng. J. 203 (2012) 43-51.

[13] Q. Liu, L. Wang, C. Wang, W. Qu, Z. Tian, D. Wang, B. Wang, Z. Xu, H. Ma, Appl. Catal., B. 136-137 (2013) 210-217.

[14] J. Okal, M. Zawadzki, Appl. Catal, B. 105 (2011) 182-190.

[15] J. Okal, M. Zawadzki, L. Krajczyk, Catal. Today. 176 (2011) 173-176.

[16] W. Walerczyk, M. Zawadzki, Catal. Today. 176 (2011) 159-162.

[17] A.E. Galetti, M.F. Gomez, L.A. Arrua, M. C. Abello, Appl. Catal. A. 408 (2011) 78-86.

[18] B.K. Vu, M.B. Song, I.Y. Ahn, Y.W. Suh, W.I. Kim, H.L. Koh, Y.G. Choi, E.W. Shin, D. J. Suh, Appl. Catal. A. 400 (2011) 25-33.

405 [19] J.P. Poupelin, G.S. Rut, F. Blanpin, G. Narcisse, G.U. Ernouf, R. Lakroix, Eur. J. Med.
406 Chem. 13 (1978) 67.
407 [20] J.J. Omolo, M.M. Johnson, S.F.V. Vuuren, C.B.D. Koning, Bioorg. Med. Chem. Lett. 21
408 (2011) 7085-7088.
409 [21] K. Chibale, M. Visser, D.V. Schalkwyk, P.J. Smith, A. Saravanamuthu, A.H. Fairlamb,
410 Tetrahedron. 59 (2003) 2289-2296.
411 [22] R. Fre´de´rick, S. Robert, C. Charlier, J. Wouters, B. Masereel, L. Pochet, J. Med. Chem.
412 50 (2007) 3645-3650.
413 [23] P.D. Re , L. Sagramora , V. Mancini , P. Valenti, L. Cima, J. Med. Chem. 13 (1970) 527-
414 531.
415 [24] R.C. Gadwood, B.V. Kamdar, L.A.C. Dubray, M.L. Wolfe, M.P. Smith, W. Watt, S.A.
416 Mizsak, V.E. Groppi, J. Med. Chem. 36 (1993) 1480-1487.
417 [25] G.W. Rewcastle, G.J. Atwell, L. Za, B.C. Baquley, W.A.J. Denny, Med. Chem. 34 (1991)
418 217-222.
419 [26] S.A. Hilderbrand, R. Weissleder, Tetrahedron Lett. 48 (2007) 4383-4385.
420 [27] S.M. Hasan, M.M. Alam, A. Husain, S. Khanna, M. Akhtar, M.S. Zaman, Eur. J. Med.
421 Chem. 44 (2009) 4896-4903.
422 [28] L. Tang, J. Yu, Y. Leng, Y. Feng, Y. Yang, R. Ji, Bioorg. Med. Chem. Lett. 13 (2003)
423 3437-3440.
424 [29] E. Tyrrell, K.H. Tesfa, I. Greenwood, A. Mann, Bioorg. Med. Chem. Lett. 18 (2008) 1
425 237-1240.
426 [30] K. Hajela, R.S. Kapil, Eur. J. Med. Chem. 32 (1997) 135-142.
427 [31] E.C. Horning, M.G. Horning, J. Org. Chem. 11 (1946) 95-99.

[32] G. Cravotto, A. Demetri, G.M. Nano, G. Palmisano, A. Penoni, S. Tagliapietra, Eur. J. Org. Chem. 2003 (2003) 4438-4444.

[33] J.T. Li, Y.W. Li, Y.L. Song, G. F. Chen, Ultrason. Sonochem. 19 (2012) 1-4.

[34] D.H. Jung, Y.R. Lee, S.H. Kim, W.S. Lyoo, Bull. Korean Chem. Soc. 30 (2009) 1989-1995.

[35] A. Ilangovan, S. Malayappasamy, S. Muralidharan, S. Maruthamuthu, Chem. Cent. J. 5 (2011) 81-86.

[36] L.L. Bin, J.T. Shou, H.L. Sha, L. Meng, Q. Na, L.T. Shuang, E-J. Chem. 3 (2006) 117-121.

[37] K.P. Nandre, V.S. Patil, S.V. Bhosale, Chin. Chem. Lett. 22 (2011) 777-780.

[38] M.T. Maghsoodlou, S.M.H. Khorassani, Z. Shahkarami, N. Maleki, M. Rostamizadeh, Chin. Chem. Lett. 21 (2010) 686-689.

[39] V.K. Rao, M.M. Kumar, A. Kumar, Indian J. chem. 50B (2011) 1128-1135.

[40] Fan, X. Sen, Li, Y.Z. Zhang, X.Y. Hu, X.Y. Wang, J. Ji, Chin. J. Org. Chem. 25 (2005) 1482-1486.

[41] S. Kantevari, R. Bantu, L. Nagarapu, J. Mol. Catal. A: Chem. 269 (2007) 53-57.

[42] Zhang, Y. Sun, C. Liang, J. Shang, Zhicai, Chin. J. Chem. 28 (2010) 2255-2259.

[43] G. Sabitha, K. Arundhathi, K. Sudhakar, B.S. Sastry, J.S. Yadav, Synth. Commun. 38 (2008) 3439-3446.

[44] N.N. Pesyan, V. Golsanamloo, S. Ganbari, E. Sahin, Tetrahedron Lett. 53 (2012) 4096-4099.

[45] B.S. Kuarm, J.V. Madhav, Y.T. Reddy, S.V. Laxmi, P.N. Reddy, B. Rajitha, P.A. Crooks, Synth. Commun. 41 (2011) 1719-1724.

[46] F. He, P. Li, Y. Gu, G. Li, Green Chem. 11 (2009) 1767-1773.

[47] X. Wang, D. Shi, Y. Li, H. Chen, X. Wei, Z. Zong, Synth. Commun. 35 (2005) 97-104.

[48] P. Zhang, Y.D. Yu, Z. H. Zhang, Synth. Commun. 38 (2008) 4474-4479.

[49] E. Yoshioka, S. Kohtani, H. Miyabe, Angew. Chem. Int. Ed. 50 (2011) 6638-6642.

[50] L. Nagarapu, B. Sridhar, S. Karnakanti, R. Bantu, Synth. Commun. 42 (2012) 967-974.

[51] D.L. Ge, Y.J. Fan, C.L. Qi, Z.X. Sun, J. Mater. Chem. A. 1 (2013) 1651-1658.

[52] A.E. Giannakas, T.C. Vaimakis, A.K. Ladavos, P.N. Trikalitis, P.J. Pomonis, J. Colloid Interface Sci. 259 (2003) 244-253.

[53] W. Aiqinga, C. Zhaolib, W. Jinga, L. Jiangqiaoa, J. Tongshoua, Chem. J. Internet. 9 (2007) 43.

Tables

Table 1. Synthesis of 2,2'-arylmethylene bis (3-hydroxy-2cyclohexene-1-one) and 2,2'-arylmethylene bis (3-hydroxy-5,5-dimethyl-2cyclohexene-1-one) - 2

Table 2. Synthesis of 1-Oxo-hexahydroxanthenes - 2 Table 3. Comparison of the effect of reaction conditions on the yield of 1-Oxo-hexahydroxanthenes - 3

Table 4. Comparison of the activity of the catalysts for the synthesis of 1-Oxo-hexahydroxanthenes - 3

Table 5. Effect of solvent on the synthesis of 1-Oxo-hexahydroxanthenes - 3

Table 6. Effect of catalyst amount on the synthesis of 1-Oxo-hexahydroxanthenes - 4

476
477
478
479
480
481
482
483
484
485
486
487
488
489
490
491
492
493
494
495
496
497
498
499
500
501

Table 1. Synthesis of 2,2'-arylmethylene bis (3-hydroxy-2cyclohexene-1-one) and 2,2'-arylmethylene bis (3-hydroxy-5,5-dimethyl-2cyclohexene-1-one)

Sl. No.	R	R_1	Product	Reaction time (min)/yield	M. P. (° C)	
					Observed	Reported
1	H	H	3a	20/ 98	215	210 - 211 (Ref 36)
2	H	4 - NO_2	3b	10/ 98	196	195 - 196 (Ref 36)
3	H	4 - Cl	3c	10/ 98	202	202 - 204 (Ref 39)
4	H	4 - OH	3d	15/ 95	202	200 - 205 (Ref 53)
5	H	3 - Cl	3e	15/ 95	190	187 - 191 (Ref 53)
6	H	3 - NO_2	3f	12/ 95	198	196 - 198 (Ref 53)
7	CH_3	H	3g	20/ 93	192	189 - 190 (Ref 33)
8	CH_3	3 - NO_2	3h	12/ 98	190	190 - 191 (Ref 33)
9	CH_3	4 - OCH_3	3i	15/ 96	142	140 - 141 (Ref 33)
10	CH_3	4 - NO_2	3j	15/ 90	190	188 - 189 (Ref 33)
11	CH_3	4 - Cl	3k	10/ 97	140	137 - 138 (Ref 33)
12	CH_3	4 - OH	3l	15/ 96	200	202 - 204 (Ref 38)

Table 2. Synthesis of 1-Oxo-hexahydroxanthenes

Sl. No.	R	R_2	Product	Reaction time (min)/yield	M. P. (° C)	
					Observed	Reported
1	H	H	5a	15/ 98	230	226 (Ref 43)
2	H	3- OCH_3	5b	14/ 93	229	-
3	H	3- OCH_2CH_3	5c	15/ 92	221	-
4	H	5 - Br	5d	10/ 98	235	236 - 238 (Ref 50)
5	H	5 - NO_2	5e	13/98	242	245 - 246 (Ref 47)
6	CH_3	H	5f	15/ 92	203	204 (Ref 43)
7	CH_3	3- OCH_3	5g	14/ 89	230	229 - 231 (Ref 48)
8	CH_3	3- OCH_2CH_3	5h	15/ 88	170	-
9	CH_3	5 - Br	5i	14/ 99	252	252 - 254 (Ref 50)
10	CH_3	5 - NO_2	5j	10/98	206	205 - 207 (Ref 47)

Table 3. Comparison of the effect of reaction conditions on the yield of 1-Oxo-hexahydroxanthenes

Sl. No.	Catalyst	Reaction time (min)	Yield (%)

1	Without catalyst	125	90
2	Bulk $ZnAl_2O_4$ (90 mg)	90	89
3	Nano $ZnAl_2O_4$ (90 mg)	15	98

Reaction Conditions: salicylaldehyde+1,3-cyclohexanedione (1:2 mole ratio), solvent = 5 mL ethanol, temperature = 80 °C.

Table 4. Comparison of the activity of the catalysts for the synthesis of 1-Oxo-hexahydroxanthenes

Sl. No.	Catalyst	Amount of catalyst	Reaction time	Yield (%)	Reference
1	$CeCl_3.7H_2O$	Catalytic amount*	1.5 – 5 h	82 - 96	43
2	TEBA[a]	100 mg	3 – 5 h	85 - 95	47
3	TCT[b]	40 mg	2 – 3 h	89 - 95	48
4	Nano $ZnAl_2O_4$	90 mg	10 -15 min	88 - 98	Our work

[a] triethylbenzylammoium chloride, [b] 2,4,6-trichloro-1,3,5-triazine

* Amount is not given

Table 5. Effect of solvents on the synthesis of 1-Oxo-hexahydroxanthenes

Sl. No.	Solvent	Yield (%)
1	Ethanol	98
2	THF	75

3	Acetonitrile	74
4	Toluene	70

Sl. No.	Catalyst amount (mg)	Yield (%)
1	90	98 (15 min)
2	60	89 (30 min)
3	50	86 (90 min)

5	Water	60

Reaction Conditions: salicylaldehyde+1,3-cyclohexanedione (1:2 mole ratio), nano $ZnAl_2O_4$ = 90 mg, solvent = 5 mL ethanol, temperature = 80 °C. Reaction time = 15 min.

Table 6. Effect of catalyst amount on the synthesis of 1-Oxo-hexahydroxanthenes

Reaction Conditions: salicylaldehyde+1,3-cyclohexanedione (1:2 mole ratio), catalyst = nano $ZnAl_2O_4$, solvent = 5 mL ethanol, temperature = 80 °C. Reaction time = 15 min - 90 min.

555
556
557
558
559
560
561
562
563
564
565
566
567
568
569
570
571
572
573
574
575
576
577
578
579
580

581

582

583

584

585

586

587

588 **Figures**

589 Fig. 1. Powder XRD pattern of bulk $ZnAl_2O_4$ (a) and nano $ZnAl_2O_4$ (b) - 2

590 Fig. 2. Powder XRD pattern of fresh nano $ZnAl_2O_4$ (a) and nano $ZnAl_2O_4$ after 10 cycles (b)
591 - 3

592 Fig. 3. FTIR spectra of bulk $ZnAl_2O_4$ (a) and nano $ZnAl_2O_4$ (b) - 4

593 Fig. 4. TEM images of nano $ZnAl_2O_4$ taken and the inset is electron diffraction pattern - 5

594 Fig. 5. Particle size distribution of nano $ZnAl_2O_4$ obtained by TEM - 6

595 Fig. 6. Energy Dispersive X-ray Analysis (EDX) spectrum of nano $ZnAl_2O_4$ - 7

596 Fig. 7. TG-DTA curves of Metal nitrate-citrate with acrylamide precursor - 8

597 Fig. 8. NH_3-TPD Pattern of nano $ZnAl_2O_4$ - 9

598 Fig. 9. CO_2-TPD Pattern of nano $ZnAl_2O_4$ - 10

599 Fig. 10. Reusability of $ZnAl_2O_4$ - 11

600

601

602

603

604

605
606
607
608
609
610
611
612
613
614
615
616
617
618
619
620
621
622
623
624
625
626
627
628
629
630

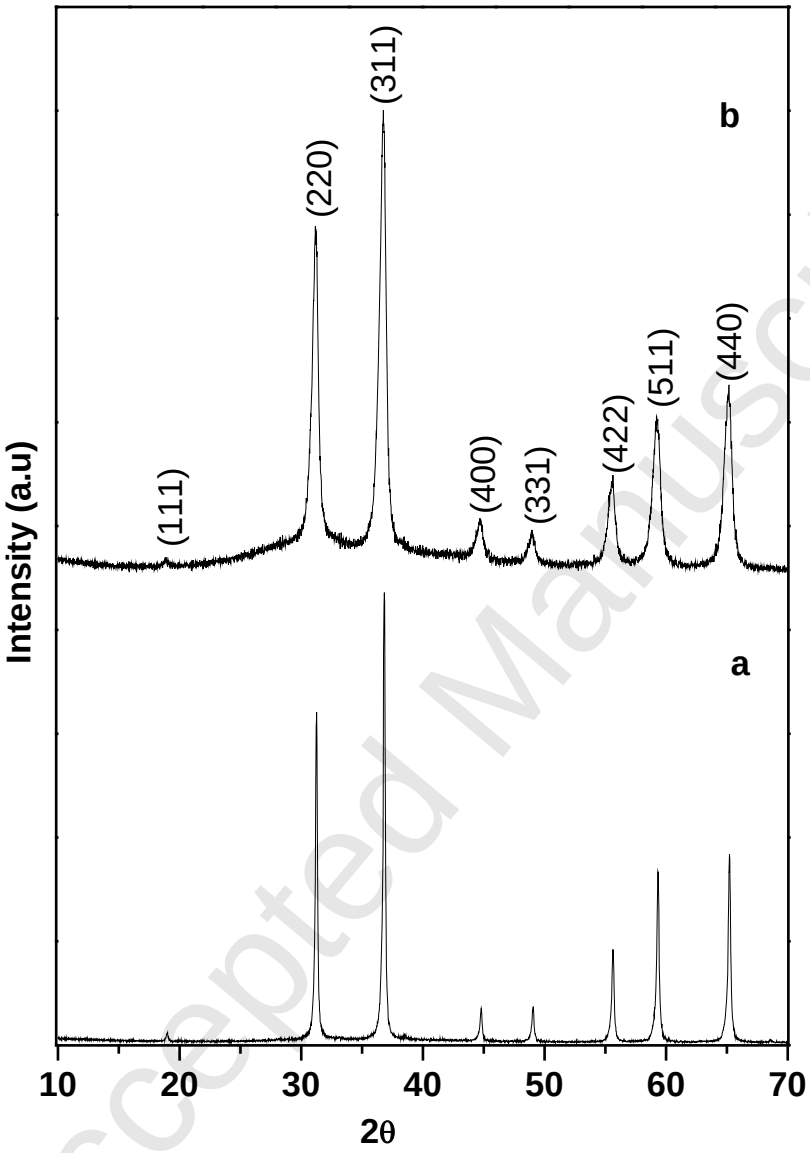

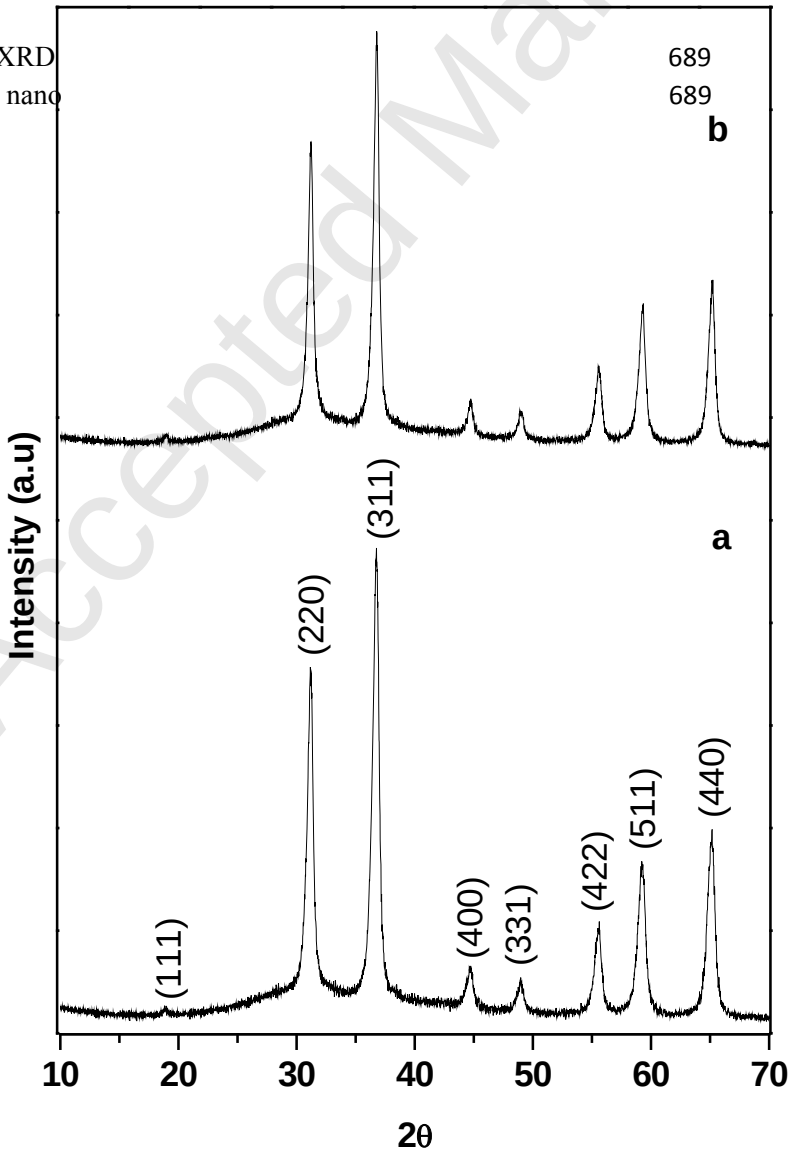

Fig. 1. Powder XRD pattern of bulk $ZnAl_2O_4$ (a) and nano $ZnAl_2O_4$ (b)

721
722
723
724
725
726
727
728
729
730
731
732
733
734
735
736
737
738
739
740
741
742
743
744
745
746

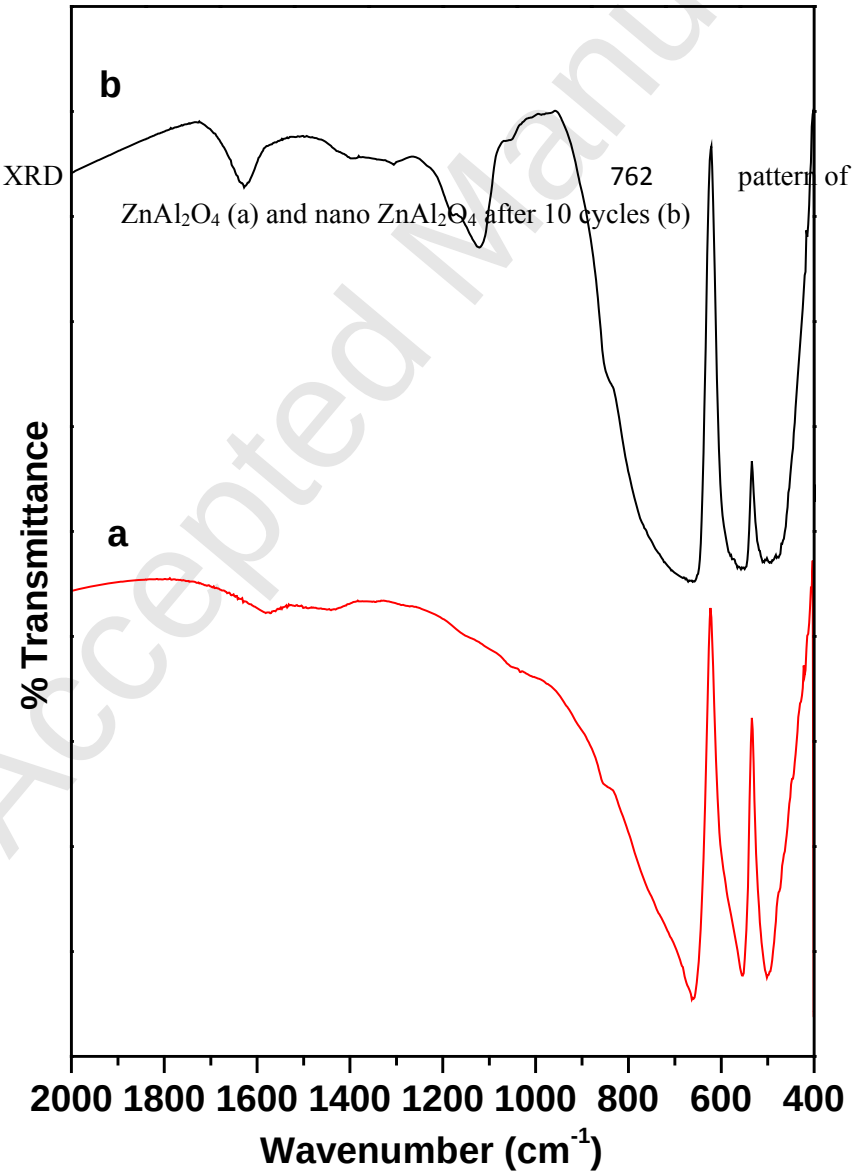

Fig. 2. Powder XRD pattern of fresh nano $ZnAl_2O_4$ (a) and nano $ZnAl_2O_4$ after 10 cycles (b)

793
794
795
796
797
798
799
800
801
802
803
804
805
806
807
808
809
810
811
812
813
814
815
816
817
818

Fig. 3. FTIR spectra of bulk $ZnAl_2O_4$ (a) and nano $ZnAl_2O_4$ (b)

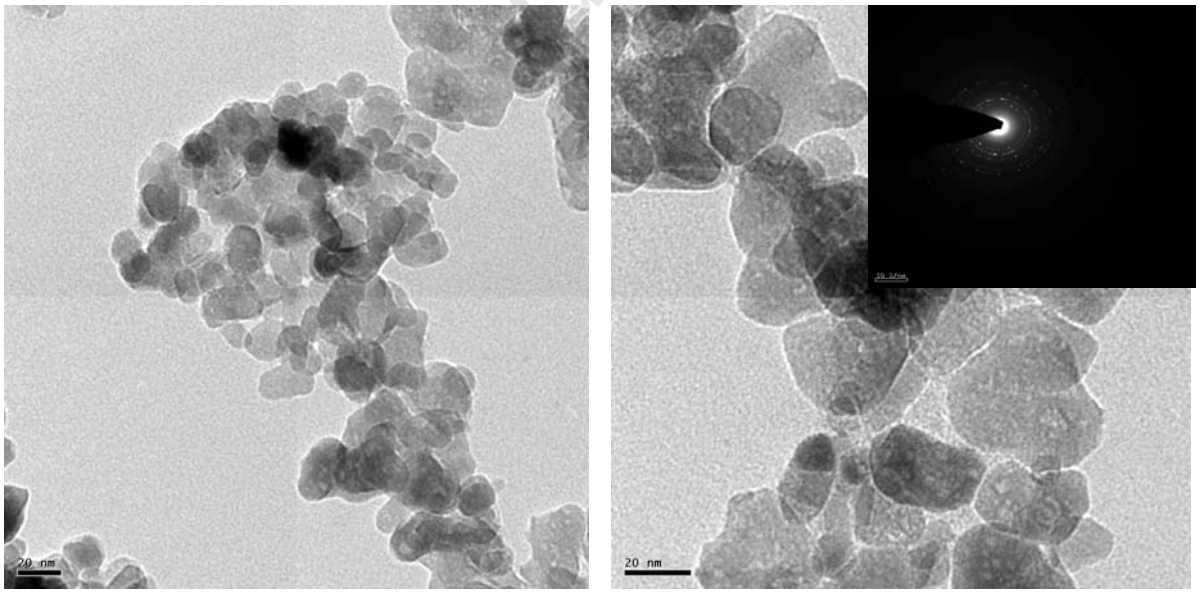

Fig.4. TEM images of nano $ZnAl_2O_4$ taken and the inset is electron diffraction pattern.

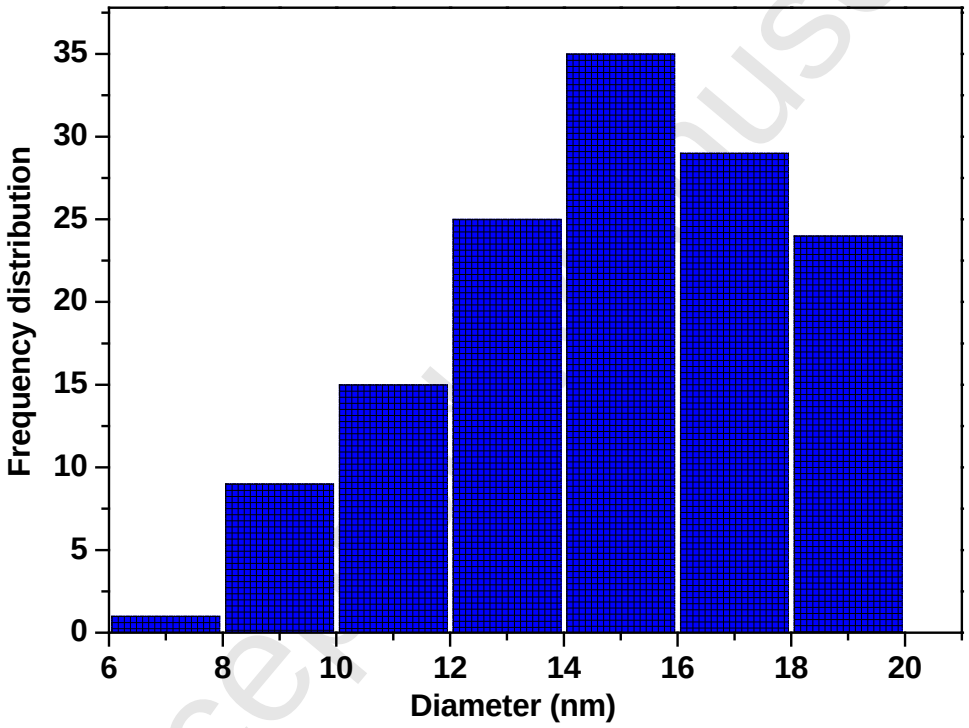

Fig.5. Particle size distribution of nano $ZnAl_2O_4$ obtained by TEM

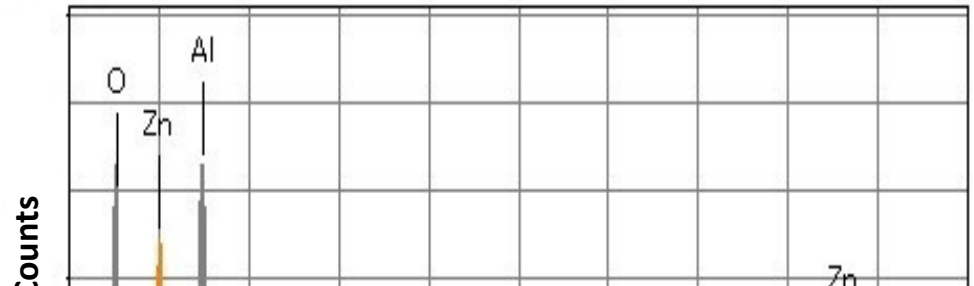

Fig. 6. Energy Dispersive X-ray Analysis (EDX) spectrum of nano $ZnAl_2O_4$

964
965
966
967
968
969
970
971
972
973
974
975
976
977
978
979
981
983
985
987
989
991
993
995
997
999

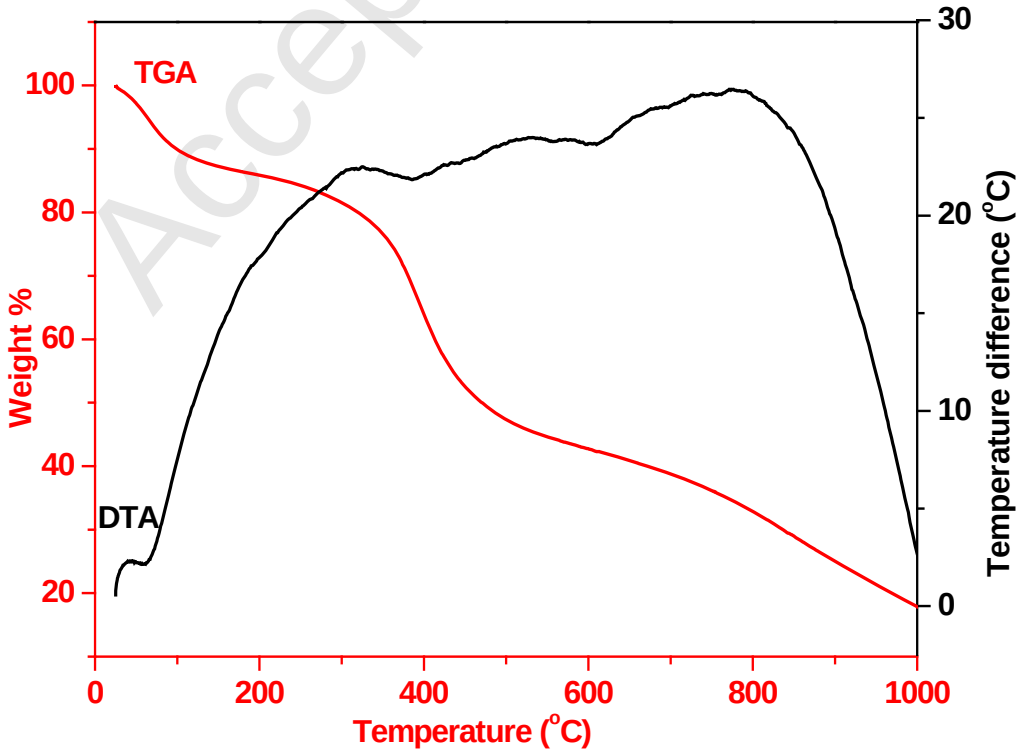

Fig. 7. TG-DTA curves of Metal nitrate-citrate with acrylamide precursor

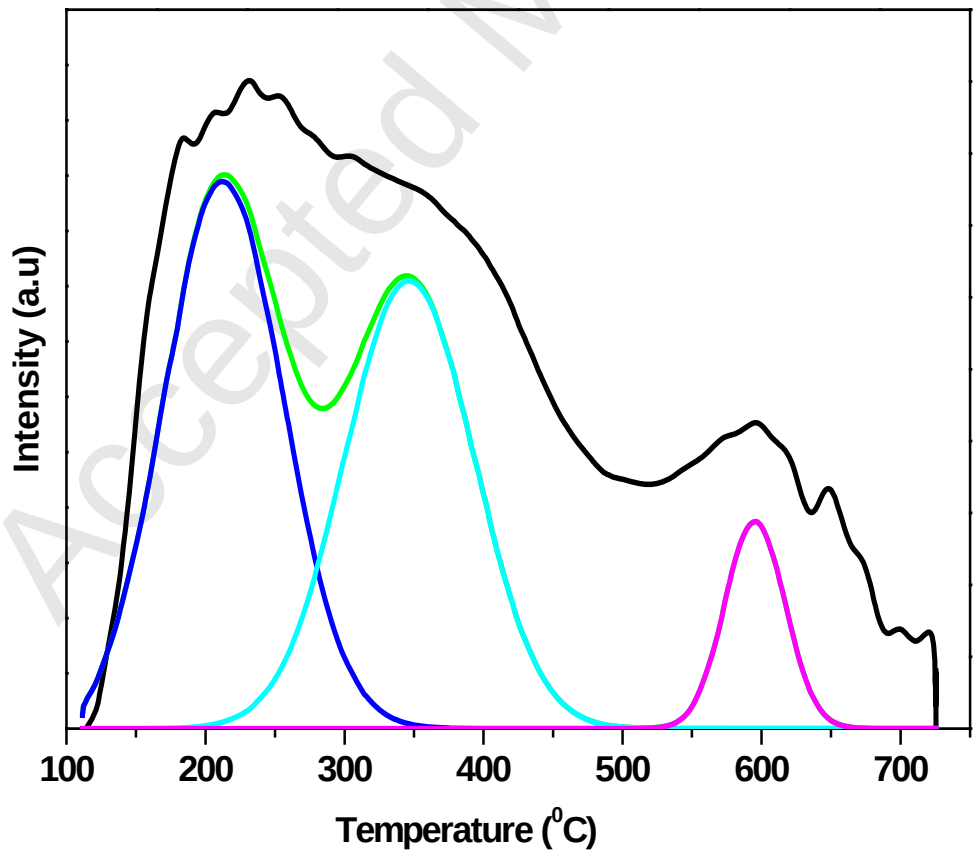

Fig. 8. NH_3-TPD pattern of nano $ZnAl_2O_4$

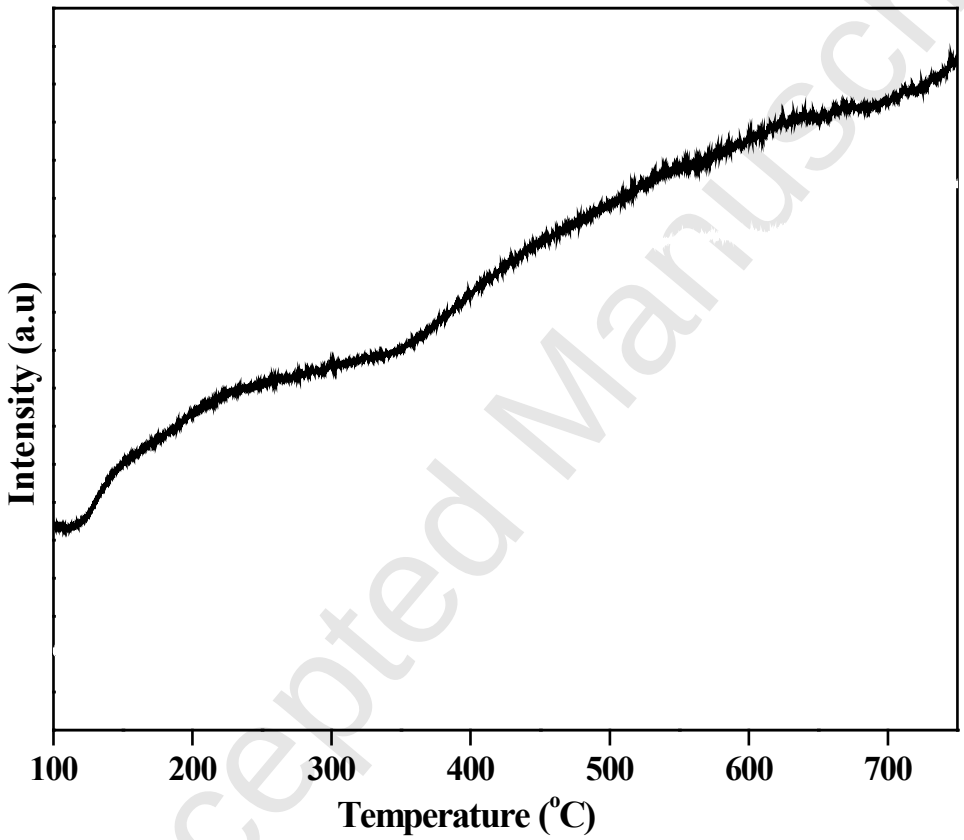

Fig. 9. CO_2-TPD pattern of nano $ZnAl_2O_4$

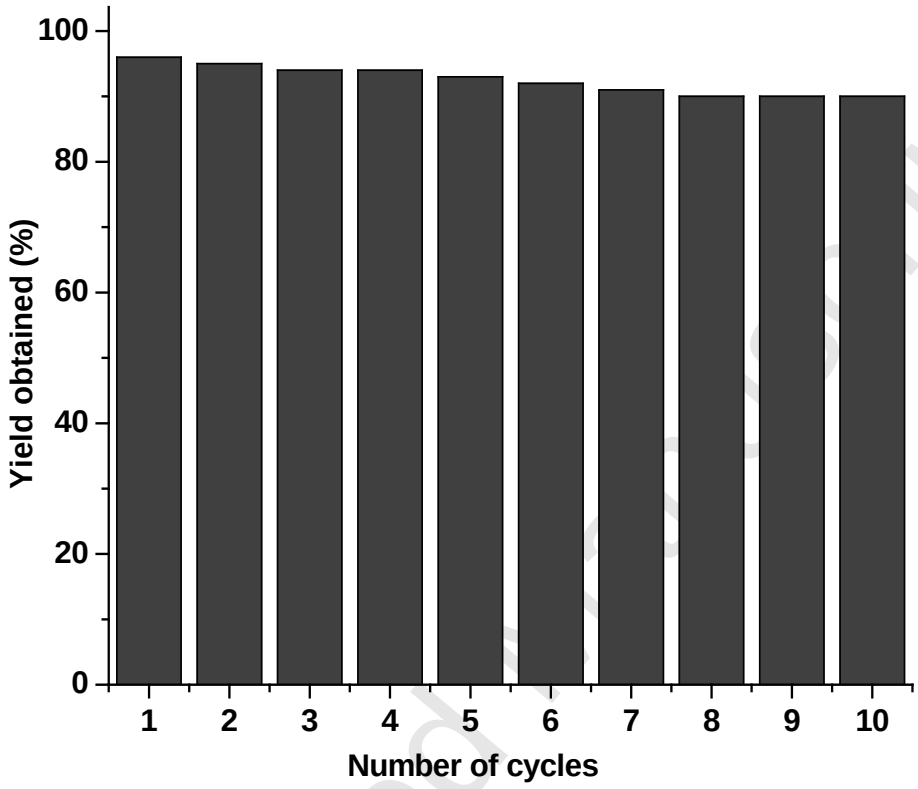

Fig. 10. Reusability of nano $ZnAl_2O_4$ for 1-Oxo-hexahydroxanthenes synthesis using salicylaldehyde and 1,3-cyclohexanedione.